

# A regularization method in the electromagnetic inverse scattering problem\*

XIONG Xiaoyun, ZHAO Yanwen\*\* and NIE Zaiping

(School of Electronic Engineering, University of Electronic Science and Technology of China, Chengdu 610054, China)

Accepted on October 18, 2006

**Abstract** Based on the normalization of measurement data equations of the inverse scattering problem, a new regularization matrix is proposed. It can eliminate the unfavorable effects caused by difference of distances between field-point or source-point and target region, reduce the loss of useful information in regularization procedure, and decrease condition numbers of the ill-posed problems. Inversion for conductivity distribution of two-dimensional axisymmetric inhomogeneous media is carried out by combining this new regularization method with distorted Born iterative method. Simulation results show that compared with the conventional method, the new regularization method is of better stability, quicker convergence, higher accuracy of inversion and higher resolution.

**Keywords:** inverse scattering, regularization, distorted Born iterative method.

The difficulties of resolving inverse scattering problem are caused by intrinsic nonlinear and ill-posed properties. The former can be solved by using linear approximation and iteration optimization, and the latter can usually be solved by using Tikhonov's method<sup>[1]</sup>. Both linear inversion<sup>[2-5]</sup> and nonlinear inversion<sup>[6-14]</sup> methods dealing with nonlinear feature of inverse scattering problem have already been widely and deeply investigated. Linear inversion method is only suitable for inverting a weak scattering object because it does not account for multiple scattering caused by the object. It is necessary for inverting the strong scattering target to employ the nonlinear inversion method that accounts for multiple scattering.

Up to now, in contrast to the nonlinear problem method processing inverse scattering, a little research work has been done in regularization method to eliminate the ill-posed property in the inverse scattering problem and its practical application procedure. In this paper, therefore, we address briefly on the nonlinear integral equation in two-dimensional axisymmetric inhomogeneous media and its discretization, and then propose a new regularization matrix, and also carry out inversion for conductivity distribution of two-dimensional axisymmetric inhomogeneous media by using distorted Born iterative method (DBIM)<sup>[2-5]</sup>.

## 1 Nonlinear electromagnetic integral equation in two-dimensional axisymmetric inhomogeneous medium

In an axisymmetric inhomogeneous medium, a coaxial loop antenna generates a pure transverse electric (TE) wave in an axisymmetric medium. Assuming that a loop antenna with radius  $\rho_t$  carries an electric current  $I$  and is located at  $z = z_t$  with time harmonic dependence  $e^{-j\omega t}$ , the partial differential equation for the electric field can be derived as

$$\left( \frac{\partial}{\partial \rho} \frac{1}{\rho} \frac{\partial}{\partial \rho} \rho + \frac{\partial^2}{\partial z^2} + k^2 \right) E_\varphi = -j\omega\mu I \delta(\rho - \rho_t) \delta(z - z_t), \quad (1)$$

where  $k = \omega \sqrt{\mu\epsilon}$  is the wave number of the medium,  $\mu$  the magnetic conductivity (in this paper, the vacuum magnetic conductivity  $\mu_0$  is chosen),  $\tilde{\epsilon} = \epsilon(\rho, z) - j\sigma(\rho, z)/\omega$  is the complex dielectric constant, in which  $\epsilon$  is a dielectric constant and  $\sigma$  is the distribution of electric conductivity of medium. By reciprocity theorem of Green's function and Eq. (1), we can derive the nonlinear integral equation for the electric field as

$$\begin{aligned} E_\varphi(\rho, z; \rho_t, z_t) &= E_\varphi^{\text{inc}}(\rho, z; \rho_t, z_t) \\ &+ k_0^2 \int_{-\infty}^{\infty} dz' \int_0^\infty d\rho' G_b(\rho', z'; \rho, z) \\ &\cdot E_\varphi(\rho', z'; \rho_t, z_t) O(\rho', z'), \end{aligned} \quad (2)$$

\* Supported by National Natural Science Foundation of China (Grant No. 60571002)

\*\* To whom correspondence should be addressed. E-mail: ywzhao@uestc.edu.cn

where  $k_0$  is wave number in vacuum,  $G_b(\rho', z'; \rho, z)$  the Green's function in the background medium, and incident electric field  $E_\varphi^{\text{inc}}(\rho, z; \rho_t, z_t)$  is

$$E_\varphi^{\text{inc}}(\rho, z; \rho_t, z_t) = j\omega\mu_0 IG_b(\rho, z; \rho_t, z_t). \quad (3)$$

The unknown object function  $O(\rho, z)$  is defined as

$$O(\rho, z) = [\tilde{\epsilon}(\rho, z) - \tilde{\epsilon}_b(\rho, z)] / \epsilon_0, \quad (4)$$

where  $\epsilon_0$  is a vacuum dielectric constant.

In order to solve the nonlinear integral equation (2) for the unknown object function  $O(\rho, z)$ , the Born's approximation is applied to linearize the nonlinear integral equation (2). In other words, in each iteration the electric field  $E_\varphi$  in the integrand of Eq. (2) is approximated as the incident field in the background medium,

$$E_\varphi(\rho, z; \rho_t, z_t) \approx E_\varphi^{\text{inc}}(\rho, z; \rho_t, z_t). \quad (5)$$

Thus, nonlinear integral Eq. (2) can be approximated as the following linear integral equation:

$$\begin{aligned} E_\varphi(\rho, z; \rho_t, z_t) - E_\varphi^{\text{inc}}(\rho, z; \rho_t, z_t) \\ \approx k_0^2 \int_{-\infty}^{\infty} dz' \int_0^{\infty} d\rho' G_b(\rho', z'; \rho, z) \\ \cdot E_\varphi^{\text{inc}}(\rho', z'; \rho_t, z_t) O(\rho', z'), \end{aligned} \quad (6)$$

where  $k_0 = \omega \sqrt{\mu_0 \epsilon_0}$ . Solving linear Eq. (6) by DBIM<sup>[8,9]</sup>, the distribution  $\tilde{\epsilon}(\rho, z)$  in the target region can be obtained.

## 2 Regularization procedure and the inverse scattering problem solving

In the given scattering data  $E_\varphi^{\text{scat}} = E_\varphi - E_\varphi^{\text{inc}}$ , dividing target region into  $N_p$  sub-regions and expanding object function  $O(\rho, z)$  by proper basis function series, the linear integral equation (6) can be discretized into a matrix equation<sup>[8,9]</sup> as

$$\mathbf{A} \cdot \mathbf{x} = \mathbf{b}, \quad (7)$$

in which  $\mathbf{x}$  is the object function vector with  $N_p$  elements,  $\mathbf{b}$  a vector with  $N_m$  measurement data,  $\mathbf{A}$  a matrix of dimension  $N_m \times N_p$ .

Inverse scattering problem described by Eq. (7) is always ill-posed. In order to obtain the stable solution of Eq. (7), the regularization method, which is usually used to circumvent the instability of inverse scattering problem, can convert solving matrix equation (7) into solving an optimization problem, i. e. solving the minimum value of cost function  $C(\mathbf{x})$ . The commonly adopted cost function  $C(\mathbf{x})$  of Tikhonov's regularization method is defined as follows:

$$C(\mathbf{x}) = \|\mathbf{b} - \mathbf{A} \cdot \mathbf{x}\| + \gamma \|\mathbf{R} \cdot \mathbf{x}\|, \quad (8)$$

where  $\gamma$  and  $\mathbf{R}$  are regularization parameter and regularization matrix, respectively. By minimizing the cost function in Eq. (8), one can obtain the following matrix equation:

$$(\mathbf{A}^* \cdot \mathbf{A} + \gamma \mathbf{R}^* \cdot \mathbf{R}) \cdot \mathbf{x} = \mathbf{A}^* \cdot \mathbf{b}, \quad (9)$$

where superscript  $*$  denotes the transposed complex conjugate of a matrix, and the matrix equation (9) can be solved by the conjugate gradient method (CGM).

The regularization method, which can suppress the impact of noise (measurement error or calculation error) on the reconstructed profile, is used to smooth target's profile that will be reconstructed. Regularization parameter  $\gamma$  is such a parameter which adjusts the effects of the regularization term (i. e., the second term on the left side of Eq. (13)), and the choice of regularization parameter  $\gamma$  is very important. In order to obtain a stable solution,  $\gamma$  must be large enough to ensure filtering out instable components (corresponding to high frequencies in spatial spectrum or detail properties in space); but,  $\gamma$  cannot be too large to avoid filtering out too many useful frequency components in the solution and thus ensure the accuracy and resolution of reconstruction. In practice, regularization parameter  $\gamma$  is chosen by numerical simulation and prior knowledge about target's profile. For example, take  $\gamma$  as a certain multiple of the first diagonal element or the maximum diagonal element in the matrix  $\mathbf{A}^* \cdot \mathbf{A}$ <sup>[10,11]</sup>. The commonly used regularization matrix  $\mathbf{R}$  is just a unit diagonal matrix of dimension  $N_p \times N_p$ , which means that each sub-region of target region has the same absolute smoothing value. In such a case, for a given regularization parameter  $\gamma$ , it may take place that useful frequencies are filtered out from some sub-regions, while instable components remained in the other ones, which will lead to obviously decreasing of the accuracy and resolution of reconstructed target's profile. The matrix  $\mathbf{R}^* \cdot \mathbf{R}$  has been chosen as the diagonal matrix of  $\mathbf{A}^* \cdot \mathbf{A}$  in Ref. [15], because it includes information about background medium and the distances from measurement point or/and source point to target's region, the choice of regularization parameter  $\gamma$  becomes easier (regularization parameter  $\gamma$  may be taken as 0.1 for all of different background medium and their measurement points, and position of source) and better reconstructed results are obtained.

In a practical measurement procedure, distances

from position of the different field point and source point to target's region may varies greatly (especially, in geophysical well logging, exciting coil and receiving coil only move along the borehole) so that differences between values in different rows of matrix  $\mathbf{A}$  of Eq. (7) become very large. Thus, the direct optimum process according to cost function (8) will result in serious loss or submerging of measurement information corresponding to the small elements in matrix  $\mathbf{A}$ , which leads to decreasing of the accuracy and resolution of reconstruction. For this reason, two sides of Eq. (7) are divided by the maximum element in each row in matrix  $\mathbf{A}$  and then a new equation can be obtained as follows:

$$\mathbf{P} \cdot \mathbf{x} = \mathbf{e}, \quad (10)$$

where

$$\mathbf{e}(i) = \mathbf{b}(i) / a_{\max}(i), \quad i = 1, \dots, N_m, \quad (11a)$$

$$\mathbf{P}(i, j) = \mathbf{A}(i, j) / a_{\max}(i), \quad j = 1, 2, \dots, N_p, \quad (11b)$$

$$a_{\max}(i) = \max \{ \mathbf{A}(i, j), j = 1, \dots, N_p \}, \quad i = 1, \dots, N_m. \quad (11c)$$

Since this method balances the importance for each measurement data, unfavorable impacts caused by difference of distances from field source points to target's region can be considerably reduced. By minimizing the cost function determined according to Eq. (8), one has

$$(\mathbf{P}^* \cdot \mathbf{P} + \gamma \mathbf{R}^* \cdot \mathbf{R}) \cdot \mathbf{x} = \mathbf{P}^* \cdot \mathbf{e}. \quad (12)$$

In the above-mentioned processing, the loss of information of measurement data is much smaller than that of using usual method. At the same time, this processing can reduce condition number of the ill-posed problems, improve stability and convergence of inversing scattering problem, and also increase accuracy and resolution of the inversion results.

In order to overcome defects caused by using unit diagonal regularization matrix  $\mathbf{R}$  ( $\mathbf{R}^* \cdot \mathbf{R}$  is also a unit diagonal matrix), let

$$\begin{cases} p_{\max}(i) = \max \{ (\mathbf{P}^* \cdot \mathbf{P})(i, j), j = 1, \dots, N_p \}, \\ i = 1, \dots, N_p \\ q_{\max} = \max \{ (\mathbf{P}^* \cdot \mathbf{P})(i, i) / p_{\max}(i), \\ i = 1, \dots, N_p \} \end{cases} \quad (13)$$

and define  $\mathbf{R}^* \cdot \mathbf{R}$  in formula (12) as follows:

$$(\mathbf{R}^* \cdot \mathbf{R})(i, j)$$

$$= \begin{cases} \alpha q_{\max} p_{\max}(i) + (\mathbf{P}^* \cdot \mathbf{P})(i, i), & i = j \\ 0, & i \neq j \end{cases}, \quad (14)$$

where  $\alpha$  is a proportional constant ( $0 < \alpha \leq 0.5$ ). Choosing a suitable value (recommended value is  $\alpha \approx 0.1$ ), the stability, convergence, accuracy and resolution of inversing scattering problem can be improved further. Simultaneously, the above-mentioned process can be easily applied to any inverse method (for examples, BIM, DBIM and so forth) for solving any inverse scattering problem (for example, problems of two-dimensional or three-dimensional geophysical and medical imaging).

### 3 Numerical results and discussion

The inversion for distribution of axisymmetric two-dimensional inhomogeneous media has been carried out by combining new modified regularization method together with distorted Born iterative method (so-called MR-DBIM method). And also, the new method as well as the accuracy of inversion results has been evaluated using relative residual error (RRE, Eq (15a)) between the calculated value about data of scattering field and measurement value, and relative mean square error (MSE, Eq(15b)) between the reconstructive profile of medium distribution inside the target's region and original profile.

$$\text{RRE} = \frac{\sum_{m=1}^{N_m} | (E_{\varphi}^{\text{scat}})^n - (E_{\varphi}^{\text{meas}})_m |}{\sum_{m=1}^{N_m} | (E_{\varphi}^{\text{meas}})_m |}, \quad (15a)$$

$$\text{MSE} = \sqrt{\frac{\sum_{p=1}^{N_p} | \sigma(p) - \sigma^n(p) |^2}{\sum_{p=1}^{N_p} | \sigma(p) |^2}}, \quad (15b)$$

where  $E_{\varphi}^{\text{scat}}$  is the measurement value of scattering field,  $(E_{\varphi}^{\text{scat}})^n$  the calculated value of scattering field after  $n$ th iteration,  $\sigma(p)$  the actual value of electric conductivity distribution in the  $p$ th patch of target's region, and  $\sigma^n(p)$  the reconstructed value of media distribution in the  $p$ th patch for target's region after  $n$ th iteration.

In this paper, reconstructed results are given using the data obtained by induction measurement in the geophysical well logging. In induction logging, the operation frequency is usually 20 kHz, displacement current can be neglected in this case, thus one can set relative permittivity  $\epsilon_r = 1$  and  $k^2 \approx j\omega\mu\sigma$ . In

the following examples, we can assume that conductivity of background media  $\sigma_b$  is 0.1 s/m except for borehole, and the conductivity in borehole,  $\sigma_m$ , is 0.01 s/m. The induction tool consists of one exciting coil and eight receiving coils. The ordinates of receiving coils are taken as  $z_r = z_s \pm 15.24$  cm,  $z_s \pm 30.48$  cm,  $z_s \pm 45.72$  cm and  $z_s \pm 63.50$  cm, respectively, where  $z_s$  denotes the ordinate of exciting coil. This tool is moved from 99.06 to 99.06 cm with an increment of 5.08 cm. This makes the total number of measurement data equal to 320.

Fig. 1(a) shows the original conductivity profile of the target's area with peak value 0.98 s/m and the conductivity contrast is relatively low and its profile also varies slowly. Fig. 1(b)–(e) show the inversion results and the curves of relative residual error and relative mean square error versus the iteration num-

ber. The abnormal region of resistance and target's region to be inverted are the same, which covers the area  $-30.48 \text{ cm} \leq z \leq 30.48 \text{ cm}$ ,  $25.40 \text{ cm} \leq \rho \leq 86.36 \text{ cm}$ . The target's region is divided into sub-meshes with  $12 \times 12 = 144$ . The conductivity profile is reconstructed separately by the improved regularization method and conventional regularization method combined with DBIM (shown in Fig. 1(b) and (c)). We can clearly see that the reconstructed profile (Fig. 1(b)) by our method is almost the same as the original profile, and the accuracy of reconstruction is very high. But, there are some differences between the reconstructed profile (Fig. 1(c)) by the conventional regularization method and the original profile. Comparing Fig. 1(d) with 1(e), we can see that both of RRE and MRE converge fast while the convergence error of our method is smaller than that of the conventional regularization method.

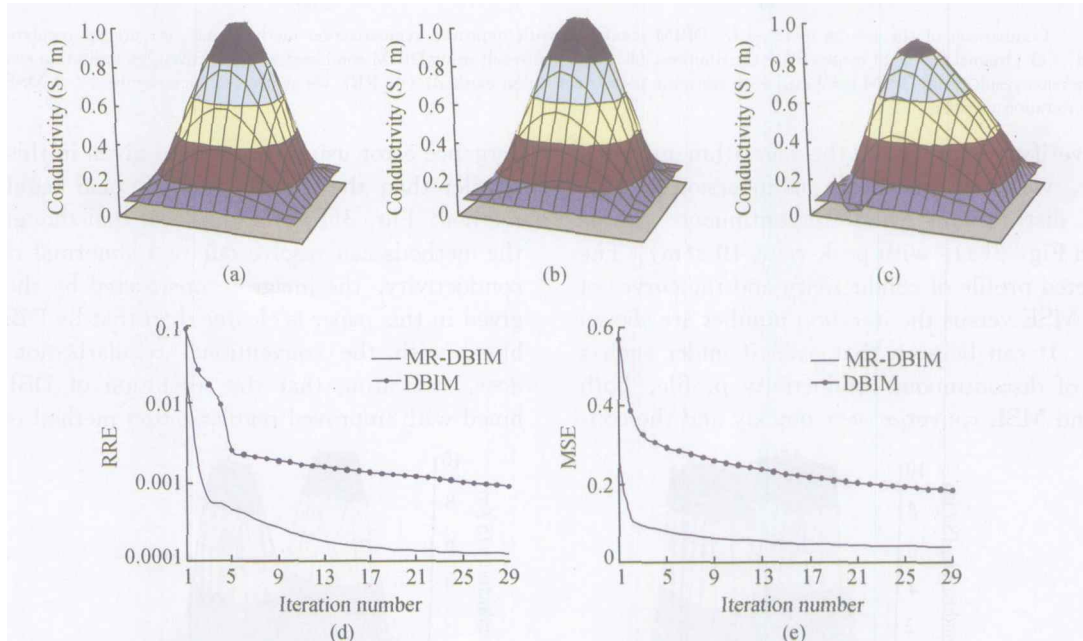


Fig. 1. Comparison of the results inverted by DBIM combined with improved regularization method and conventional regularization method, respectively. (a) Original profile of conductivity distribution; (b) inversion result using DBIM combined with improved regularization method; (c) inversion result using DBIM combined with conventional regularization method; (d) RRE versus the iteration number; (e) MSE versus the iteration number.

We have further tested the stability and convergence of our method by increasing the conductivity contrast in the condition of keeping the same shape of original conductivity profile. The peak value of profile was increased to 23.48 s/m from 0.98 s/m for the above example, and the other parameters such as inversion region and mesh division were kept the same as the above example. The similar conclusion shown in Fig. 2 has been obtained. It can be seen from Fig. 2 (d) that the amplitude of oscillation is very small by

using our method and only appears at a very small value of the RRE though there are oscillations in two curves of relative residual error, which shows that our method is more stable than the conventional method. It can also be seen that relative MSE of conductivity distribution keeps stable (shown as in Fig. 2(e)) while using both the two methods, which indicates that it is necessary to observe simultaneously the RRE variation and relative MSE in studying properties of some inverse scattering method and regularization method.

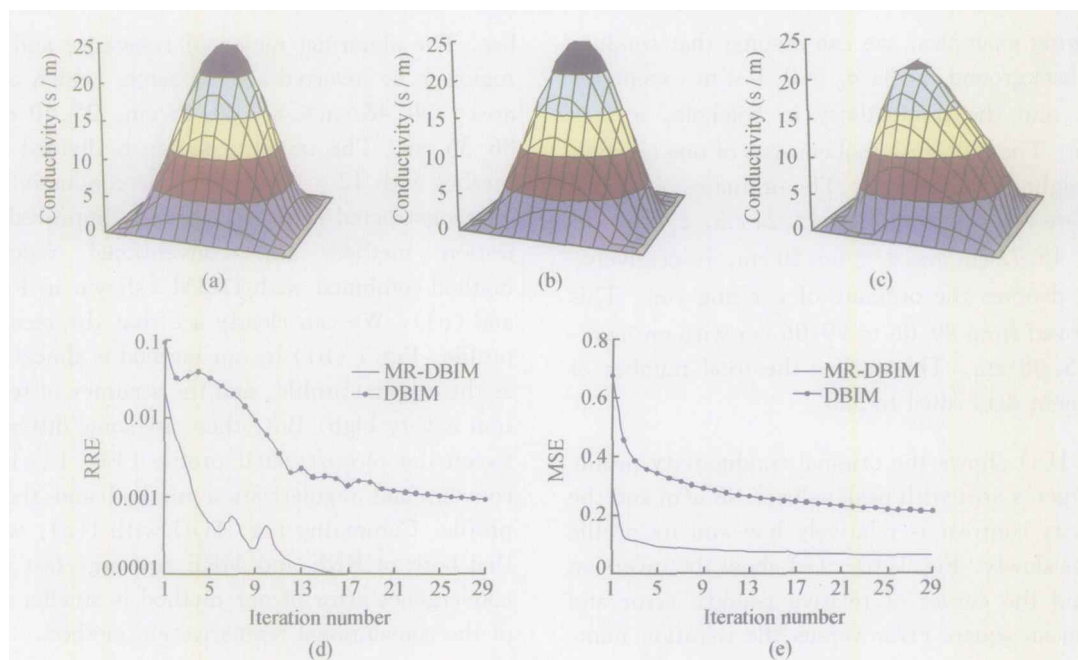


Fig. 2. Comparison of the results inverted by DBIM combined with improved regularization method and conventional regularization method. (a) Original profile of conductivity distribution; (b) inversion result using DBIM combined with improved regularization method; (c) inversion result using DBIM combined with conventional regularization method; (d) RRE versus the iteration number; (e) MSE versus the iteration number.

To verify resolution of the algorithm given in this paper, we have carried out an inversion of conductivity distribution with discontinuous profile (shown in Fig. 3(a), with peak-value 10 S/m). The reconstructed profile of conductivity and the curves of RRE and MSE versus the iteration number are shown in Fig. 3. It can be seen that even if under such a condition of discontinuous conductivity profile, both of RRE and MSE converge very quickly and the con-

vergence error using the method given in this paper is smaller than that by the conventional regularization method. Fig. 3(b) and (c) show that though both of the methods can resolve out two abnormal regions of conductivity, the image reconstructed by the method given in this paper is clearer than that by DBIM combined with the conventional regularization method, indicating that the resolution of DBIM combined with improved regularization method is higher.

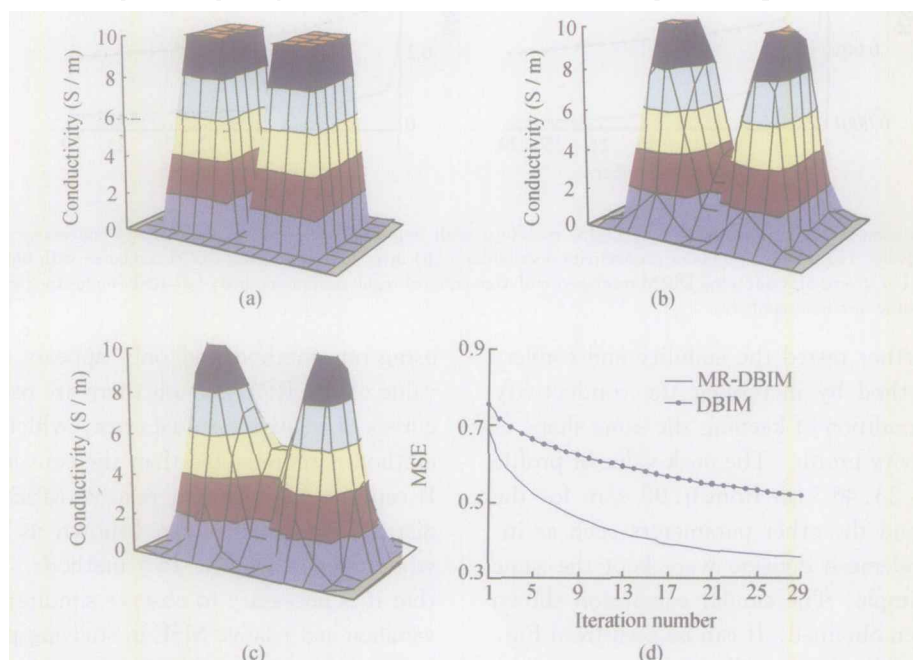


Fig. 3. Comparison of the results inverted by DBIM combined with improved regularization method and conventional regularization method. (a) Original profile of conductivity distribution; (b) inversion result of DBIM combined with improved regularization method; (c) inversion results of DBIM combined with conventional regularization method; (d) MSE versus the iteration number.

## 4 Conclusions

A new regularization matrix is described in this paper. Combining this matrix with distorted Born iterative method, the inversion for conductivity distribution of two-dimensional axisymmetric inhomogeneous media is carried out. The reconstructed examples show that the new regularization method improves the stability, convergence and the reconstructed accuracy and resolution of reconstruction significantly. In addition, construction and application of the new regularization matrix are easy. We will extend this regularization method to other inverse methods (for instance BIM method) or other applied domains (such as biomedical imaging) in the future.

## References

- 1 Twomey S. Introduction to the Mathematics of Inversion in Remote sensing and Indirect Measurements. New York: Elsevier, 1977.
- 2 Born M. and Wolf E. Principles of Optics, 6th ed. New York: Pergamon Press, 1980.
- 3 Devaney A. J. A filtered backpropagation algorithm for diffraction tomography. *Ultrasonic Imaging*, 1982, 4: 336—360.
- 4 Pichot C. and Jofre L. Active microwave imaging of inhomogeneous bodies. *IEEE Trans. Antennas. Propagat.*, 1985, 33: 416—425.
- 5 Bolomey J. C. and Pichot C. Microwave tomography: From theory to practical imaging systems. *Int. J. Imag. Sys. Tech.*, 1990, 2: 144—156.
- 6 Wang Y. M. and Chew W. C. An iterative solution of the two-dimensional electromagnetic inverse scattering problem. *Int. J. Imaging Syst. Technol.*, 1989, 1: 100—108.
- 7 Chew W. C. *Waves and Fields in Inhomogeneous Media*, 2nd ed. New York: IEEE Press, 1995.
- 8 Chew W. C. and Wang Y. M. Reconstruction of two-dimensional permittivity using the distorted Born iterative method. *IEEE Trans. Med. Imag.*, 1990, 9(2): 218—225.
- 9 Zhao Y. W. and Nie Z. P. Inversion of two-dimensional axisymmetric potential field using the distorted born iterative method. *Acta Electronica Sinica*, 1997, 25(12): 10—14.
- 10 Liu Q. H. Reconstruction of two-dimensional axisymmetric inhomogeneous media. *IEEE Trans. Geosci. Remote Sensing*, 1993, 31: 587—594.
- 11 Liu Q. H. Nonlinear inversion of electrode-type resistivity measurements. *IEEE Trans. Geosci. Remote Sensing*, 1994, 32: 499—507.
- 12 Habashy T. M., Groom R. W. and Spies B. R. Beyond the born and Rytov approximations. A nonlinear approach to electromagnetic scattering. *J. Geophys. Res.*, 1993, 98: 1759—1775.
- 13 Torres-Verdin C. and Habashy T. M. Rapid 2.5-D forward modeling and inversion via a new nonlinear scattering approximation. *Radio Sci.*, 1994, 29: 1051—1079.
- 14 Kooij J. and van der Berg P. M. Nonlinear inversion in TE scattering. *IEEE Trans. Microwave Theory Tech.*, 1998, 46(11): 1704—1712.
- 15 Cui T. J., Qin Y., Wang G. L. et al. Low-frequency detection of two-dimensional buried objects using high-order extended Born approximations. *Inverse Problems*, 2004, 20: S41—S62.